Spin-Lattice Interaction in the Quasi-One-Dimensional Helimagnet $LiCu_2O_2$

László Mihály,[1,2] Balázs Dóra,[2] András Ványolos,[2] Helmuth Berger,[3] and László Forró[3]

[1]*Department of Physics and Astronomy, Stony Brook University, Stony Brook, New York 11794-3800, USA*
[2]*Electron Transport Research Group of the Hungarian Academy of Science and Department of Physics, Budapest University of Technology and Economics, 1111 Budapest, Hungary*
[3]*EPFL, Lausanne, CH-1015 Switzerland*

(Received 1 February 2006; published 11 August 2006)

The field dependence of the electron spin resonance in a helimagnet $LiCu_2O_2$ was investigated for the first time. In the paramagnetic state, a broad resonance line was observed corresponding to a g factor of 2.3. In the critical regime, around the paramagnetic to helimagnetic phase transition the resonance broadens and shifts to higher frequencies. A narrow signal is recovered at a low temperature, corresponding to a spin gap of 1.4 meV in zero field. A comprehensive model of the magnons is presented, using exchange parameters from neutron scattering [T. Masuda *et al.* Phys. Rev. B **72**, 014405 (2005)] and the spin anisotropy determined here. The role of the quantum fluctuations is discussed.

DOI: 10.1103/PhysRevLett.97.067206 PACS numbers: 75.30.Ds, 75.25.+z, 75.50.−y

Ground state solutions of the antiferromagnetic Heisenberg model range from the Néel state to valence bond solids and resonating valence bonds, depending on the interactions, the dimensionality and connectivity of the system, and other factors [1,2]. When the ground state has long range Néel order, the excitation spectrum is gapless at $q = 0$. This follows from the rotational invariance of the Hamiltonian: The creation of long wavelength excitations, where the relative angle of the neighboring spins changes only by an infinitesimal amount, costs very little energy. Gapless excitations, on the other hand, cause strong quantum fluctuations, suppressing or destroying the Néel state [3]. The spin-orbit coupling leads to new terms in the Hamiltonian, including the single ion anisotropy, the exchange anisotropy, the Dzyaloshinskii-Moriya coupling, and others. The coupling between the direction of the spins and the lattice removes the rotational invariance in many real materials, creates a gap in the spin wave spectrum, and contributes to the stability of the quasiclassical ground state.

In this work, we investigated the magnetic excitations in a quasi-one-dimensional helimagnet, $LiCu_2O_2$, in fields of 0–14 T and at temperatures 2.5–60 K. The main result is that in the ground state two of the three magnon branches are gapped with $\Delta = 11.7\ \mathrm{cm}^{-1} = 1.4$ meV. Our calculations reveal that this gap is due to a spin-lattice coupling of $D = 0.083$ meV. We show that the proper treatment of the helical order of the spins explains the order-of-magnitude difference between the coupling parameter and the gap, enabling this weak coupling to reduce the quantum fluctuations significantly. $LiCu_2O_2$ crystallizes in an orthorhombic structure with the space group $Pnma$ and lattice constants $a = 5.730$ Å, $b = 2.86$ Å, and $c = 12.417$ Å [4]. The Cu^{2+} ions carry magnetic moments with spin 1/2, and they form quasi-one-dimensional chains with zigzag "ladders" along the b direction (Fig. 1). The material has two characteristics relevant to frustrated quantum magnets: The exchange interaction goes beyond the first neighbors, and the structure has a triangular motif susceptible to frustration.

Quantum effects and fluctuations are expected to be important since the spins are 1/2 and the system is quasi-one-dimensional. Indeed, in an early work, Zvyagin *et al.* interpreted the broadening and disappearance of the ESR signal in terms of a "dimer liquid" state below the 24 K phase transition [5]. However, instead of a quantum liquid state, NMR, μSR, and neutron scattering results revealed a quasiclassical helical spin order along the chains, with a wave vector $\mathbf{Q}$ incommensurate to the lattice [6–9]. All spins were found to be parallel to the a-b plane. In the $\mathbf{q} = \pm\mathbf{Q}$ region, the "acoustic" magnon branches were observed, but the energy resolution was not sufficiently high to exclude or measure a possible gap [10]. ESR has the resolution to address this question, and the application of the external static magnetic field can be used to explore the spin dynamics further. Note that in ESR the magnetic

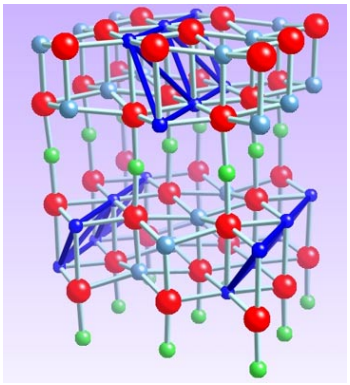

FIG. 1 (color online). Crystal structure of $LiCu_2O_2$, based on Ref. [4]. The magnetic Cu^{2+} ions (connected in zigzag fashion) are dark blue, the nonmagnetic copper (between the layers) is green, the lithium (within the layers) is light blue, and the oxygen (denoted by the large bubbles) is red. The dark blue bonds emphasize the triangular spin ladder.

excitation is at $\mathbf{q} = \mathbf{0}$, but in the presence of a magnetic superlattice it couples to the modes at $\mathbf{q} = \pm\mathbf{Q}$ as well.

The measurements were performed on an oriented single crystal sample of dimensions 3 mm × 6 mm × 0.5 mm. According to the Laue diffractogram, the c axis is along the shortest dimension of the sample; the a and b directions are parallel to the edges of the slab. There is a twinning in the a-b plane, as is typical of most $LiCu_2O_2$ samples. Spin resonance was detected in the transmission of the far infrared light, measured at Stony Brook University's high magnetic field or infrared facility at the U12 IR beam line of the National Synchrotron Light Source. The light propagated parallel to the static magnetic field and passed through the sample along the c direction. The polarization of the incident light was controlled and set to several directions within the a-b plane.

Figure 2 shows the temperature dependence of the spin resonance at 12 T field. The raw transmission curves were normalized to the transmission of the sample in 0 T at 25 K, when no spin resonant absorption is expected. The oscillations seen in the baseline of the frequency dependence are residuals of the interference fringes seen in the raw spectra. These fringes are common and well understood for samples of plane-parallel geometry.

At high temperatures, a broad resonance at the "free spin" frequency of $\hbar\omega = g\mu_B H$ with a g factor of $g = 2.3$ is observed. The ESR line starts to broaden below 30 K; all of this is in agreement with earlier ESR investigations [5,11,12]. In the critical regime around 22–24 K, the ESR line is about 3–4 T broad (full width at half maximum), and it shifts to a higher frequency. Below 15 K, a narrower signal is recovered at a markedly higher frequency. This signal, characteristic to the development of a spin gap in the ordered phase, has not been seen in earlier spin resonance works [5,11,12], due to limitations in accessible fields and frequencies in those studies. Measurements at several other fields (8, 10, and 14 T) yielded results qualitatively similar to the behavior presented in Fig. 2 and will be published elsewhere. Choi *et al.* suggested a transition from helimagnetic to Néel order [13] at $T = 9$ K, but there is no indication of a change in the ESR signal in that range.

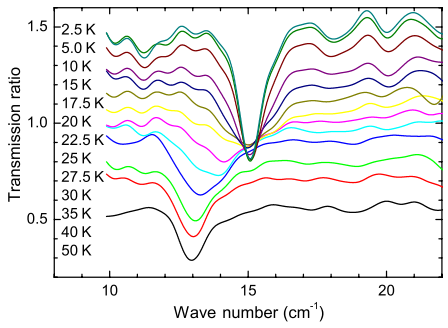

FIG. 2 (color online). Temperature dependence of the ESR signal at 12 T magnetic field. The measured transmissions, relative to the transmission in zero field, 25 K, are shown. Colors indicate the temperature.

Zvyagin and co-workers measured ESR in the paramagnetic state at 277 GHz (9.2 cm^{-1}) [5]. They observed the broadening and disappearance of the ESR signal, interpreting it in terms of the formation of a spin singlet liquid state above the ordering temperature. In fact, as our data show, the integrated intensity of the signal remains approximately constant as we cross the phase transition temperature. Vorotynov *et al.* observed an "antiferromagnetic resonance" (AFMR) signal at ~30 GHz (1 cm^{-1}) [11,12] in zero field, with an unexpected and unexplained magnetic field dependence and anisotropy. There is no information about the intensity of this signal relative to the ESR in the paramagnetic state. However, since nearly all of the spectral weight of the paramagnetic resonance remains in the high field or frequency range studied here, the AFMR signal at 1 cm^{-1} must be relatively weak and may be related to low energy processes that are secondary to the physics of this material.

Figure 3 shows the field dependence of the spin resonance at low temperatures. The three data sets in the upper panel correspond to the different polarization states of the incident light. Each set of curves was obtained by dividing the measured spectrum with a reference spectrum recorded at a temperature above the phase transition in zero external field. The resonance line shapes, frequencies, and the intensities are similar for all three polarization states. The zero-field resonance at 11.7 cm^{-1} is visible in two of the data sets. The most striking feature is the dramatic increase of the resonant absorption at higher magnetic fields.

To extract the field dependence of the resonant frequency, we took the average of the three sets of data and assembled an intensity map (Fig. 4). In terms of simple, two-sublattice antiferromagnets, both the intensity and the

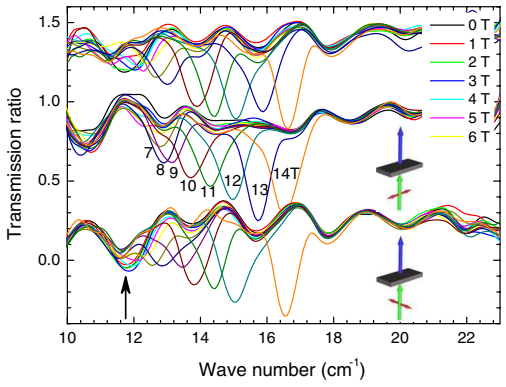

FIG. 3 (color online). Field dependence of the transmission at 2.5 K. The three sets of curves represent the transmission relative to the transmission at high temperature and zero field. Top: Partially polarized light, relative to 25 K. Middle: Light polarized parallel to the long axis of the sample, relative to 20 K. Bottom: Polarization along the short axis, relative to 25 K. The black arrow emphasizes the nonvanishing spin resonance line intensity at 11.7 cm^{-1} in zero field.

field dependence are surprising. The intensity of the antiferromagnetic resonance should have a very weak field dependence [14] only. More importantly, the typical field dependence of the resonance frequency in antiferromagnets ($\omega \propto \sqrt{H^2 + H_0^2}$) cannot be fitted to the data without residual systematic deviations.

The model used for the magnon spectrum [10] was adopted to evaluate the results presented in Fig. 3. We extended it to finite magnetic fields perpendicular to the plane of the spins and added the terms responsible for the spin gap. The Hamiltonian is

$$\mathcal{H} = \sum_{i,j} J_1 S_{i,j} S_{i+1,j} + J_2 S_{i,j} S_{i+2,j} + J_4 S_{i,j} S_{i+4,j} + J_\perp S_{i,j} S_{i,j+1} - g\mu_B H S^y_{i,j} + D_{\mathrm{ex}} S^y_{i,j} S^y_{i+1,j}. \quad (1)$$

The indices i and j run along and perpendicular to the double chains, respectively. J_1 is the coupling between along the diagonal "rungs" of the ladder, J_2 and J_4 are the nearest neighbor and the second neighbor couplings along the chain, and $J_\perp$ is the interchain coupling. The "easy plane" is represented by the exchange anisotropy of $D_{\mathrm{ex}} < 0$ (the negative D_{ex} is required because the orientation of the nearest neighbor spins has an antiferromagnetic character). Following conventions established in the literature [15,16], the reference frame for the spin components is selected so that the magnetic field H is applied along the y directions and in zero field the spins are in the x-z plane (i.e., the crystallographic c direction is parallel to the y axis). In finite magnetic field, the spin directions are on a cone whose axis is parallel to y.

The ground state and the spin wave excitations of this model were found with the methods described in Refs. [10,15–17]. Following "model 1" of Masuda *et al.* [10], we used $J_1 = 6.4$ meV, $J_2 = -11.9$ meV, $J_4 = 7.6$ meV, and $J_\perp = 1.8$ meV, and in zero field and with no anisotropy we reproduced the fits to the published spin wave spectrum. After carefully tracing the factor 2's, we believe that the coupling constants published in the preprint version of Ref. [10] were correct.

In general, a helical spin arrangement possesses 3 Goldstone modes, one at $\omega(\mathbf{0})$ corresponding to the free rotation of the ordered moments within the helical plane and two degenerate ones at $\omega(\pm\mathbf{Q})$ associated with the tilting of the plane of the helix [16,18]. The easy plane anisotropy generates a finite spin gap at $\pm\mathbf{Q}$, where $\mathbf{Q} = (\pi/a, \phi/b)$ is the ordering wave vector with $\phi = 5.2$ rad (the angle between subsequent spins on the same leg of the ladder). In terms of the Fourier transform of the exchange interaction $J_{\mathbf{q}} = 2[J_1 \cos(bq_b/2) + J_2 \cos(bq_b) + J_4 \cos(2bq_b) + J_\perp \cos(aq_a)]$, the gap is $\Delta = 2S\sqrt{J' \cos(\phi/2) D_{\mathrm{ex}}}$, where the effective exchange coupling is defined as $J' = (J_{2\mathbf{Q}} + J_{\mathbf{0}})/4 - J_{\mathbf{Q}}/2$.

The application of external magnetic field tilts the spins out of the x-z plane and lifts the degeneracy of the $\pm\mathbf{Q}$ points, resulting in distinct spin gaps and different spin susceptibilities (Fig. 4). The angle α to the y axis is determined from $\cos\alpha = g\mu_B H/[2S(D_{\mathrm{ex}} + J_{\mathbf{0}}/2 - J_{\mathbf{Q}}/2)]$. The magnon spectrum is $\omega(\mathbf{k}) = \sqrt{(A_{\mathbf{k}} + A_{-\mathbf{k}})^2 - 4B_{\mathbf{k}}^2} + A_{\mathbf{k}} - A_{-\mathbf{k}}$, where the spin resonance frequencies are obtained by substituting $\mathbf{k} = \pm\mathbf{Q}$. Here we used

$$A_{\mathbf{k}} = \frac{S}{2}\Big(\frac{H}{S}\cos(\alpha) + D_{\mathrm{ex}}[\sin^2(\alpha)\cos(bk_y) - 2\cos^2(\alpha)] + \frac{1}{4}[J_{\mathbf{k}+\mathbf{Q}}(1+\cos(\alpha))^2 + J_{\mathbf{k}-\mathbf{Q}}(1-\cos(\alpha))^2] + \sin^2(\alpha)(J_{\mathbf{k}}/2 - J_{\mathbf{Q}}) - \cos^2(\alpha)J_{\mathbf{0}}\Big),$$

$$B_{\mathbf{k}} = \frac{S}{2}\Big(\frac{\sin^2(\alpha)}{4}[J_{\mathbf{k}+\mathbf{Q}} + J_{\mathbf{k}-\mathbf{Q}} - 2J_{\mathbf{k}}] - D_{\mathrm{ex}}\sin^2(\alpha)\cos(bk_y)\Big). \quad (2)$$

The continuous lines in the figure represent the center frequencies of the two branches generated by the application of the external field. The strength of the resonance line was set according to the calculated spin susceptibility, and lifetime effects were simulated by Lorentzian line shapes of 0.1 meV relaxation rate, independent of field. On the lower branch, the strong absorption at high fields gradually

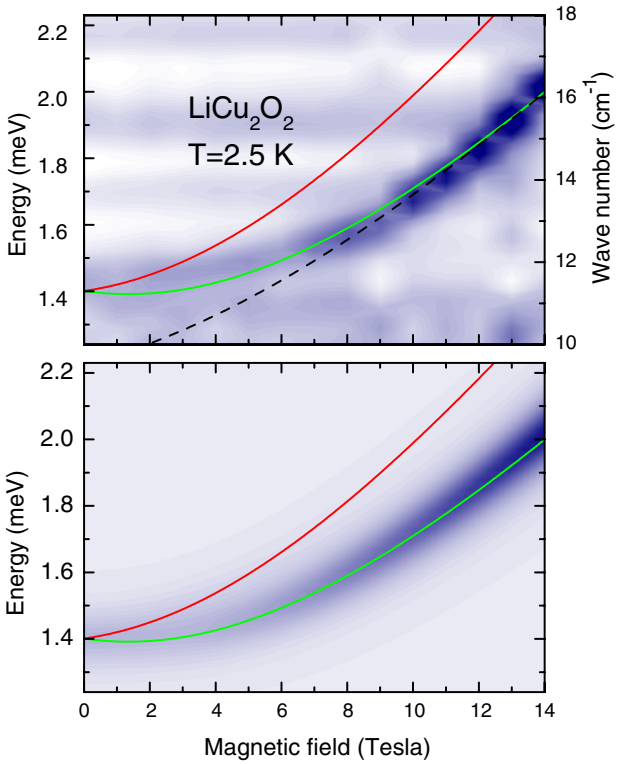

FIG. 4 (color online). Upper panel: Intensity map based on the average of the three data sets shown in Fig. 3. Lower panel: Intensity map generated from the calculated frequencies and susceptibilities, based on "model 1" described in the text. The continuous and dashed lines represent the resonance frequencies corresponding to two models under consideration.

decreases as the field is lowered, due to the field dependence of the susceptibility. The susceptibility belonging to the upper branch is so small that the corresponding resonance signal is below the noise level.

In order to obtain the near-perfect agreement with the experiment, we adjusted two parameters: the magnitude of the anisotropy $D = D_{\rm ex}\cos(\phi/2) = 0.083$ was set to reproduce the zero-field gap, and the g factor was $g = 1.85$. Instead of using an exchange anisotropy in Eq. (1), one may use single ion anisotropy or Dzyaloshinskii-Moriya interaction, with very similar results [19]. The microscopic origin of all of these interactions is the spin-orbit coupling, but *ab initio* calculations are difficult. Moriya [20] estimated the anisotropic component of the exchange interaction in the order of $D \sim (\Delta g/g)^2 J$, where Δg is the g-factor shift in the paramagnetic state and $\Delta g/g$ is a measure of the spin-orbit coupling. A spin-lattice coupling in the range of $D \sim 100$ μeV is therefore consistent with the g factor ranging between 1.95 and 2.3 in the paramagnetic state [11,12]. The energy gap scales linearly with the spin-orbit and exchange couplings, $\Delta \sim (\Delta g/g)J$.

Neutron scattering results would be consistent with a different set of exchange parameters (called "model 2" in Ref. [10]), characterized by large antiferromagnetic J_1 and J_2 ($J_1 = 105.5$ meV, $J_2 = 33.8$ meV, $J_4 = -1.6$ meV, and $J_\perp = 0.23$ meV). It was impossible to get adequate fits to the observed field dependence of the gap in this model. For example, with $D = 0.0088$ meV one can match the high field behavior (see the dashed line in Fig. 4), but at low fields the calculation misses the experiment (see also Fig. 3) entirely.

Quantum fluctuations suppress the sublattice magnetic order by the amount of $\Delta S = \int \frac{g(\mathbf{q})}{\omega(\mathbf{q})} d^d q$ [here d is the dimensionality of the lattice, $\omega(\mathbf{q})$ is the magnon excitation energy at wave vector $\mathbf{q}$, and $g(\mathbf{q})$ is expressed in terms of $J(\mathbf{q})$] [3,16]. With no spin-lattice coupling, we obtained $\Delta S = 0.150$, a 30% drop relative to spin $S = 1/2$, which is to be contrasted with $\Delta S = 0.197$ for a two-dimensional antiferromagnet. In the presence of the easy plane term, the corresponding value is $\Delta S = 0.125$. The coupling to the lattice makes the quasiclassical state more stable. Further reduction of ΔS is seen in the presence of the static magnetic field. Further evidence for reduced sublattice magnetization follows from the g factor determined in the fit. The macroscopic energy scale of the interaction with the magnetic field is determined by the product $g\mu_B H S_{\rm eff}$. In our treatment, the quantum effects were neglected, and instead of a reduced S the quantum correction appears as a reduction of g.

In conclusion, we established that the spin wave spectrum of $LiCu_2O_2$ has a gap of 1.4 meV and interpreted the experiments in terms of a model including an easy plane anisotropy. This term in the Hamiltonian accounts for the experimentally observed spin direction in the crystallographic a-b plane, and it also contributes to the stability of the quasiclassical ground state. There are intriguing possibilities for similar measurements on helimagnets with an external field applied in the plane of the spin rotation. The theoretical methods applied in this work cannot be readily adapted to this new configuration. It is known that the static spin order turns into a soliton lattice [21,22], but calculations for the ESR excitations have not been performed yet.

We are indebted to Jessica Thomas for the x-ray work, to G. L. Carr for developing the IR facilities at U12IR, to K. Holczer for continued discussions and support, and to A. Jánossy for consultations on the technical and theoretical aspects of ESR. B. D. acknowledges the Magyary program (MZFK) for support. Financial support of the Hungarian Research Funds No. OTKA TS049881 and No. NDF45172 is acknowledged. The work in Lausanne was supported by the Swiss NSF and its NCCR "MaNEP." Use of the National Synchrotron Light Source, Brookhaven National Laboratory, was supported by the U.S. Department of Energy, Office of Science, Office of Basic Energy Sciences, under Contract No. DE-AC02-98CH10886.

[1] For a historical introduction, see Claire L'huillier, cond-mat/0502464.
[2] P. Lemmens, G. Güntherodt, and C. Gros, Phys. Rep. **375**, 1 (2003).
[3] P. W. Anderson, Phys. Rev. **86**, 694 (1952); R. Kubo, Phys. Rev. **87**, 568 (1952).
[4] R. Berger, P. Önnerud, and R. Tellgren, J. Alloys Compd. **184**, 315 (1992).
[5] S. Zvyagin *et al.*, Phys. Rev. B **66**, 064424 (2002).
[6] A. A. Gippius *et al.*, Phys. Rev. B **70**, 020406(R) (2004).
[7] B. Roessli *et al.*, Physica (Amsterdam) **296B**, 306 (2001).
[8] T. Masuda *et al.*, Phys. Rev. Lett. **92**, 177201 (2004).
[9] S.-L. Drechsler *et al.*, Phys. Rev. Lett. **94**, 039705 (2005); T. Masuda *et al.*, Phys. Rev. Lett. **94**, 039706 (2005).
[10] T. Masuda *et al.*, Phys. Rev. B **72**, 014405 (2005) (see also cond-mat/0412625).
[11] A. M. Vorotynov *et al.*, Zh. Eksp. Teor. Fiz. **113**, 1866 (1998) [JETP **86**, 1020 (1998)].
[12] A. M. Vorotynov *et al.*, J. Magn. Magn. Mater. **188**, 233 (1998).
[13] K.-Y. Choi, S. A. Zvyagin, G. Cao, and P. Lemmens, Phys. Rev. B **69**, 104421 (2004).
[14] D. Talbayev, L. Mihály, and J. Zhou, Phys. Rev. Lett. **93**, 017202 (2004).
[15] T. Nagamiya, in *Solid State Physics*, edited by F. Seitz, D. Turnbull, and H. Ehrenreich (Academic, New York, 1967).
[16] T. Ohyama and H. Shiba, J. Phys. Soc. Jpn. **63**, 3454 (1994).
[17] E. A. Turov, *Physical Properties of Magnetically Ordered Crystals* (Academic, New York, 1964).
[18] M. Y. Veillette, A. J. A. James, and F. H. L. Essler, Phys. Rev. B **72**, 134429 (2005).
[19] L. Mihály *et al.* (to be published).
[20] T. Moriya, Phys. Rev. **120**, 91 (1960).
[21] A. E. Jacobs, T. Nikuni, and H. Shiba, J. Phys. Soc. Jpn. **62**, 4066 (1993).
[22] A. Zheludev *et al.*, Phys. Rev. B **57**, 2968 (1998).